Short Article

Cell Host & Microbe

BIRC2/cIAP1 Is a Negative Regulator of HIV-1 Transcription and Can Be Targeted by Smac Mimetics to Promote Reversal of Viral Latency

Graphical Abstract

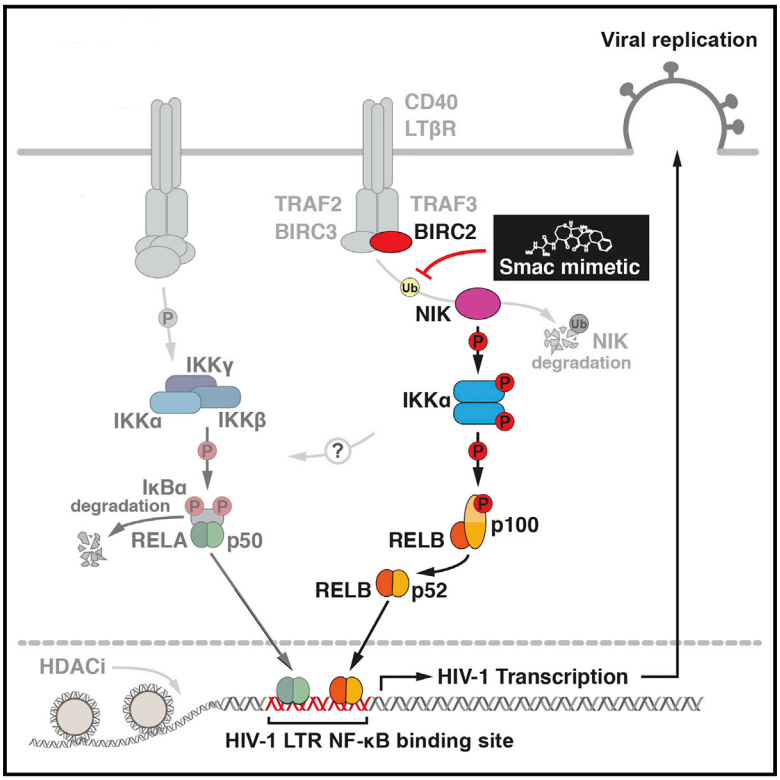

Authors

Lars Pache, Miriam S. Dutra, Adam M. Spivak, ..., John A.T. Young, Vicente Planelles, Sumit K. Chanda

Correspondence

schanda@sbpdiscovery.org

In Brief

Eradicating the latent HIV-1 reservoir represents a challenge. Pache et al. identify BIRC2/cIAP1 as a negative regulator of early HIV-1 transcription. Antagonism of BIRC2 by Smac mimetics, a class of molecules currently under evaluation for cancer, enhances HIV-1 transcription, reactivates latent virus, and synergizes with HDAC inhibitors to reverse latency.

Highlights

- Targeted RNAi screen identifies host proteins that impede early-stage HIV-1 replication
- BIRC2/cIAP1 is a negative regulator of LTR-dependent HIV-1 transcription
- BIRC2 depletion by Smac mimetic activates NF-κB signaling and reverses HIV-1 latency
- Smac mimetic and HDAC inhibitor synergize to reverse HIV-1 latency in vitro and ex vivo

Pache et al., 2015, Cell Host & Microbe *18*, 345–353
September 9, 2015
http://dx.doi.org/10.1016/j.chom.2015.08.009

CellPress

Cell Host & Microbe
Short Article

BIRC2/cIAP1 Is a Negative Regulator of HIV-1 Transcription and Can Be Targeted by Smac Mimetics to Promote Reversal of Viral Latency

Lars Pache,[1] Miriam S. Dutra,[1] Adam M. Spivak,[2] John M. Marlett,[3] Jeffrey P. Murry,[3,9] Young Hwang,[4] Ana M. Maestre,[5] Lara Manganaro,[5] Mitchell Vamos,[6] Peter Teriete,[6] Laura J. Martins,[2] Renate König,[1,7,8] Viviana Simon,[5] Alberto Bosque,[2] Ana Fernandez-Sesma,[5] Nicholas D.P. Cosford,[6] Frederic D. Bushman,[4] John A.T. Young,[3,10] Vicente Planelles,[2] and Sumit K. Chanda[1,*]

[1]Infectious and Inflammatory Disease Center, Sanford Burnham Prebys Medical Discovery Institute, 10901 North Torrey Pines Road, La Jolla, CA 92037, USA
[2]Division of Microbiology and Immunology, Department of Pathology, University of Utah School of Medicine, 15 North Medical Drive East #2100, Salt Lake City, UT 84112, USA
[3]Nomis Center for Immunobiology and Microbial Pathogenesis, The Salk Institute for Biological Studies, 10010 North Torrey Pines Road, La Jolla, CA 92037, USA
[4]Department of Microbiology, Perelman School of Medicine at the University of Pennsylvania, Philadelphia, PA 19104, USA
[5]Department of Microbiology, Icahn School of Medicine at Mount Sinai, New York, NY 10029, USA
[6]Cell Death and Survival Networks Research Program, NCI-Designated Cancer Center, Sanford Burnham Prebys Medical Discovery Institute, 10901 North Torrey Pines Road, La Jolla, CA 92037, USA
[7]Paul-Ehrlich-Institut, Paul-Ehrlich-Strasse 51-59, 63225 Langen, Germany
[8]German Center for Infection Research (DZIF), 63225 Langen, Germany
[9]Present address: Gilead Sciences, 333 Lakeside Drive, Foster City, CA 94404, USA
[10]Present address: F. Hoffmann-La Roche Ltd., Grenzacherstrasse 124, 4070 Basel, Switzerland
*Correspondence: schanda@sbpdiscovery.org
http://dx.doi.org/10.1016/j.chom.2015.08.009

SUMMARY

Combination antiretroviral therapy (ART) is able to suppress HIV-1 replication to undetectable levels. However, the persistence of latent viral reservoirs allows for a rebound of viral load upon cessation of therapy. Thus, therapeutic strategies to eradicate the viral latent reservoir are critically needed. Employing a targeted RNAi screen, we identified the ubiquitin ligase BIRC2 (cIAP1), a repressor of the noncanonical NF-κB pathway, as a potent negative regulator of LTR-dependent HIV-1 transcription. Depletion of BIRC2 through treatment with small molecule antagonists known as Smac mimetics enhanced HIV-1 transcription, leading to a reversal of latency in a JLat latency model system. Critically, treatment of resting CD4+ T cells isolated from ART-suppressed patients with the histone deacetylase inhibitor (HDACi) panobinostat together with Smac mimetics resulted in synergistic activation of the latent reservoir. These data implicate Smac mimetics as useful agents for shock-and-kill strategies to eliminate the latent HIV reservoir.

INTRODUCTION

HIV-1 latency is a state of nonproductive infection in which transcription of viral genes is repressed, likely through the concerted activities of multiple host pathways. While HIV-1 replication can be reduced to undetectable levels using combination antiretroviral therapy (ART), latently infected viral reservoirs can persist for decades (reviewed in Margolis, 2010). In well-suppressed patients, cessation of therapy typically leads to increased viremia within 3–4 weeks, and thus HIV-1-infected individuals must remain on ART throughout their lifetimes. Given the expense and toxicities associated with long-term therapies, pharmacological strategies designed to eradicate the viral latent reservoir represent a critical unmet need. Current "shock and kill" approaches seek to purge this reservoir by treating patients with therapeutics that activate latently infected cells, which are thought to be subsequently eliminated due to viral cytopathic effects or the immune response of the host (Xing and Siliciano, 2013). However, the optimal means for reactivating latent HIV-1 is at present unclear.

The establishment and maintenance of HIV-1 latency is controlled by a multitude of *cis*- and *trans*-acting mechanisms that include factors affecting the local chromatin environment or the levels of specific transcription factors, respectively (Donahue and Wainberg, 2013). Histone deacetylase inhibitors (HDACis) are known as general activators of transcription and have also been shown to reverse latency in multiple model systems (Margolis, 2011). Recent studies have indicated that most HDACi are unable to reactivate latent HIV-1 ex vivo with robust and consistent efficacies (Bullen et al., 2014; Wei et al., 2014). Therefore, it is presently not clear if treatment with an HDACi as single agent is sufficient to effectively reactivate latent HIV-1.

In addition to the local chromatin environment, specific transcription factors are also critical regulators of viral latency. A significant body of evidence indicates that NF-κB signaling plays an important role in the reactivation of latent HIV-1, implicating its regulation as an important therapeutic strategy for latency

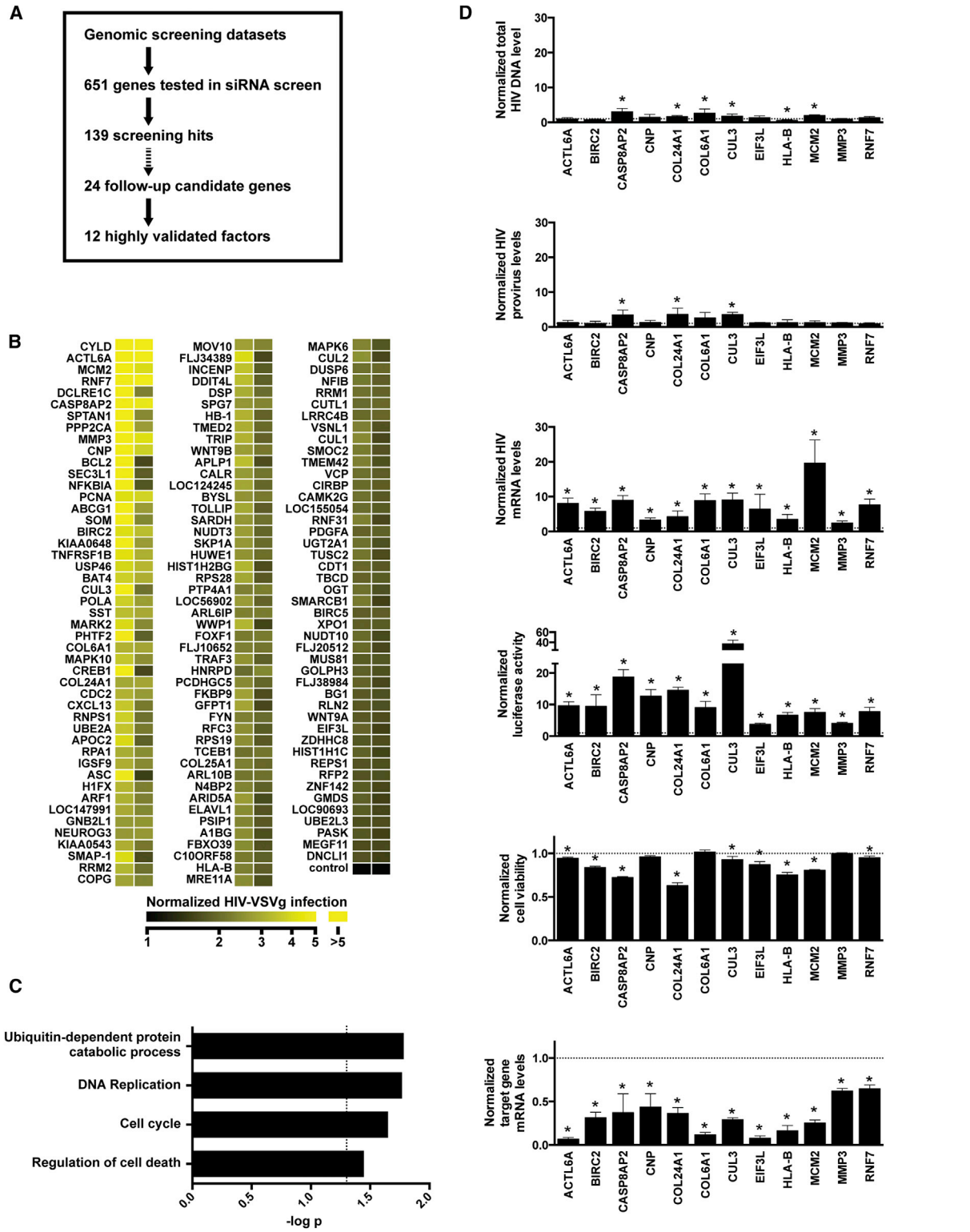

Figure 1. Identification of Cellular Factors Impeding HIV-1 Replication through Targeted siRNA Screening

(A) Candidate genes derived from genome-wide screening data sets were evaluated in a siRNA screen in HEK293T cells infected with HIV-1(VSVg). Twenty-four screening hits were selected for further validation, with 12 of these candidate genes being successfully validated using a set of more rigorous criteria (see text).

(B) Heatmap showing the activity of siRNAs targeting 139 genes identified in a siRNA screen described in (A). See also Table S1.

(C) Enrichment analysis of biological processes among screening hits. Shown are selected gene ontology terms enriched with $p < 0.05$ following Benjamini-Hochberg correction.

(legend continued on next page)

reversal (Nabel and Baltimore, 1987; Williams et al., 2006). In fact, among the most efficient proposed latency reversing agents (LRAs) are protein kinase C (PKC) activators, including bryostatin, ingenol, and phorbol esters such as PMA and prostratin. These compounds activate the canonical NF-κB pathway and have been found to reverse latency in cellular models and CD4+ T cells from HIV-1-infected patients (Bullen et al., 2014; Spivak et al., 2015; Xing and Siliciano, 2013). However, clinical uptake of these compounds has been complicated by concerns about tumorigenesis and other toxicities, particularly due to uncontrolled cytokine release (Xing and Siliciano, 2013).

Toxicity associated with agonists of canonical NF-κB signaling, which is governed by TAK1/IKK signalosome activation, is in large part due to the acute, short-lived transcriptional activation that is initiated after pathway activation, resulting in a broad inflammatory response. Although abundant evidence implicates canonical NF-κB signaling in the control of HIV-1 transcription and latency, the influence of the noncanonical NF-κB pathway in regulating HIV-1 transcription and latency has not been established. In contrast to canonical NF-κB signaling, the noncanonical NF-κB pathway is characterized by a slower onset, long-lasting transcriptional response, and higher functional selectivity, restricting its impact to a limited number of cellular processes and cell types (reviewed in Sun, 2012). The activation of the noncanonical NF-κB pathway occurs only through a specific subset of tumor necrosis factor receptors (TNFRs), including lymphotoxin beta receptor (LTβR) and CD40. In the absence of stimulation, a complex of BIRC2 (cIAP1), BIRC3 (cIAP2), TRAF2, and TRAF3 constitutively degrades NF-κB-inducing kinase (NIK). Upon receptor activation, BIRC2 and BIRC3 promote the ubiquitination and subsequent degradation of TRAF3, thereby permitting an accumulation of NIK. In turn, NIK activation results in the phosphorylation IKKα, leading to the subsequent proteolytic processing of p100 to p52. p52 forms a heterodimer with the RELB transcription factor and translocates to the nucleus, inducing the expression of target genes. Crosstalk between various canonical and noncanonical NF-κB signaling components, resulting in both positive and negative pathway crossregulation, is considered to be a critical feature in shaping biological responses to a variety of extracellular stimuli (Basak et al., 2007; Shih et al., 2011; Zarnegar et al., 2008).

Here, using targeted RNAi screening, we have identified BIRC2, a repressor of the noncanonical NF-κB pathway, as a potent regulator of HIV-1 transcription and as a therapeutic target for the reversal of latency. Small molecule antagonists of BIRC2, in combination with HDAC inhibitors, activated latent proviruses in both cell line-based models of latency and in primary CD4+ T cells isolated from ART-suppressed HIV-1-infected patients. The results of this study indicate that the pharmacological activation of the noncanonical NF-κB pathway can be used as a component of a combinatorial regimen to reactivate latent HIV-1, while potentially limiting toxicity risks associated with systemic activation of NF-κB signaling by PKC agonists.

RESULTS

Identification of Host Cell Factors that Impede Early Stages of HIV-1 Replication

Using a genome-wide siRNA-based loss-of-function screen, we previously identified 295 cellular genes encoding proteins that support viral replication (König et al., 2008). To elucidate cellular factors that interfere with HIV-1 replication, we have reanalyzed this data set along with additional published and unpublished data sets from genome-wide gain- or loss-of-function analyses (Agarwal et al., 2006; Nguyen et al., 2007), identifying 651 genes that were predicted to have a likelihood of impeding HIV-1 replication. Using a triaging strategy based on results from an arrayed siRNA loss-of-function screen (Figure 1A), we evaluated the role of these factors in the early stages of HIV-1 replication, including LTR-mediated transcription. Four distinct siRNAs targeting each candidate gene were evaluated in HEK293T cells infected with a single-cycle, VSV-G-pseudotyped, HIV-1 reporter virus (HIV-1 [VSVg]) in the absence of interferon. Results from this analysis led to the identification of 139 host factors that, when depleted, enhanced viral infection by 50% or more compared to the negative control with at least two independent siRNAs (Figure 1B; see Table S1 available online). Proteins involved in cell cycle regulation, ubiquitination, apoptosis, and DNA replication were found to be enriched in the set of 139 genes (Figure 1C), including CYLD, a gene we recently reported to regulate LTR-dependent transcription (Manganaro et al., 2014).

Cellular Factors that Limit Viral Transcription

We next performed a more rigorous validation study on 24 of the 139 factors that, when depleted, promoted HIV-1 infection. A gene was considered validated if at least two sequence-independent siRNAs enhanced expression of the luciferase reporter gene by 2.5-fold or more. We excluded genes where RNAi depletion altered cell viability >35% or the mRNA expression level of the targeted gene was not reduced by >35%. We found that 12 of the 24 selected genes met these more rigorous criteria (Table S2), including factors involved in apoptotic signaling (*BIRC2*, *CASP8AP2*), ubiquitin-mediated proteolysis (*CUL3*, *RNF7*), and antigen presentation (*HLA-B*). Only one factor induced G2/M cell cycle arrest upon depletion (Figure S1A) (Groschel and Bushman, 2005; Gummuluru and Emerman, 1999). We next used previously established assays to identify the specific steps of the early viral replication cycle that were influenced by these 12 host factors (Figures 1D and S1B). Knockdown of a subset of genes, including *CASP8AP2*, *CUL3*, and *COL6A1*, led to a modest increase in the levels of viral DNA and integrated provirus. Depletion of eight genes enhanced levels of HIV-1 transcription without significantly affecting levels of integrated provirus, among these the ubiquitin ligase *BIRC2*, a critical regulator of noncanonical NF-κB signaling.

BIRC2 Antagonist Treatment Enhances HIV-1 Infection

Smac mimetics are synthetic molecules that mimic a critical tetrapeptide sequence from the second mitochondria-derived

(D) Mapping of 12 validated genes to the HIV-1 replication cycle. HEK293T cells were treated with siRNAs targeting the indicated genes. Following infection with HIV-1(VSVg), the levels of HIV-1 total DNA, integrated provirus, and HIV-1 mRNA were determined by qPCR. Also shown are luciferase expression levels, target gene knockdown levels, and cell viability upon target gene knockdown. All values are normalized to nontargeting control siRNAs and represent mean ± SD of at least three biological replicates. * indicates statistical significance as determined by Holm-Sidak t test (alpha = 0.05).

activator of caspase (Smac/Diablo). Smac binds to the baculoviral IAP repeat (BIR) domains that are common to the eight members of the inhibitor of apoptosis (IAP) family of proteins, which includes XIAP, BIRC2, and BIRC3 (Fulda and Vucic, 2012). The IAP proteins differ in function, and only BIRC2 and BIRC3 are known regulators of noncanonical NF-κB signaling. Most Smac mimetics directly compete with caspases for XIAP binding, but also can allosterically activate the E3 ubiquitin ligase activity of BIRC2 and BIRC3, leading to autoubiquitination and subsequent degradation of these proteins. Primarily through their ability to bind XIAP, Smac mimetics can elicit proapoptotic activities, and thus have been developed to treat both solid and hematological cancers (Bai et al., 2014). We have previously described the small molecule SBI-0637142 as a potent Smac mimetic that preferentially targets BIRC2 (Finlay et al., 2014; Vamos et al., 2013). Here, we find that treating HEK293T cells with SBI-0637142 resulted in enhanced HIV-1 replication, similar to the effects of siRNA-mediated *BIRC2* knockdown. This activity was concordant with the depletion of BIRC2 protein, while no change in BIRC3 protein levels was observed (Figure 2A). Furthermore, the loss of BIRC2 led to the accumulation of NIK, indicating that treatment with the Smac mimetic resulted in the activation of the noncanonical NF-κB pathway.

Next, CD4+ T cells isolated from six healthy donors were treated with SBI-0637142 or LCL161, a second Smac mimetic that has been evaluated in phase I/II clinical trials for patients with advanced solid tumors (Bai et al., 2014; Infante et al., 2014). Treatment with SBI-0637142 and LCL161 both enhanced expression of the viral luciferase reporter gene 2- to 10-fold relative to the DMSO control upon HIV-1(VSVg) infection, without inducing significant cytotoxicity (Figure 2B). As expected, both compounds decreased BIRC2 protein levels and resulted in the stabilization of NIK.

BIRC2 Affects Viral Transcription via NF-κB-Dependent Signaling

The HIV LTR contains two copies of an NF-κB enhancer element known to bind the RELA:p50 heterodimer in response to the activation of canonical NF-κB signaling (Nabel and Baltimore, 1987). Observations using in vitro biochemical systems indicate that the noncanonical RELB:p52 heterodimers also can bind these sequences (Britanova et al., 2008; Fusco et al., 2009). Since knockdown of *BIRC2*, a negative regulator of noncanonical NF-κB signaling, increased expression of HIV-1 mRNA (Figure 2C), we hypothesized that the effects of BIRC2 depletion were mediated through NIK-dependent activation of NF-κB signaling and subsequent interaction of transcription factors with the NF-κB binding sites in the HIV-1 LTR. To test this hypothesis, siRNA-treated HEK293T cells were infected with VSV-G-pseudotyped HIV-1 that had either mutant or native NF-κB binding sites in the LTR (Figure 2D). We found that knocking down *BIRC2* by siRNA treatment had little effect on HIV-1 expression when the NF-κB binding sites were inactivated by mutation. Consistent with these findings, mutating the NF-κB binding sites in the LTR abrogated the effects of SBI-0637142 upon HIV-1 transcription (Figure 2E). Moreover, overexpression of LTβR or CD40, both members of the TNF receptor superfamily that stimulate the noncanonical NF-κB pathway, increased the expression of the viral luciferase reporter gene upon HIV-1(VSVg) infection (Figure 2F). Taken together, these results indicate that BIRC2 affects HIV-1 LTR-dependent transcription through regulation of NF-κB signaling.

BIRC2 Antagonists Act as Latency-Reversing Agents

Since transcriptional regulation has been implicated in the maintenance of HIV-1 latency, we investigated whether antagonism of BIRC2 can lead to reactivation of latent infection. Treating the latently infected Jurkat cell line JLat 10.6 with SBI-0637142 led to a dose-dependent reactivation of the provirus with negligible effects on cell viability (Figure 3A). The extent of viral latency reversal was found to be proportional to the depletion of BIRC2 and the activation of the noncanonical NF-κB pathway, as indicated by the accumulation of NIK and the processing of p100 to p52. Importantly, we found that three additional Smac mimetics, which have previously been evaluated in clinical trials (Bai et al., 2014), also showed LRA activity in a Jurkat latency model (Figure S2A). This indicates that latency reversal is not limited to individual compounds, but that Smac mimetics more generally represent a novel class of LRAs.

We also monitored the activation kinetics of NF-κB signaling upon treatment with SBI-0637142. After exposing JLat cells to the Smac mimetic, we observed degradation of BIRC2 within 15 min, followed by the stabilization of NIK after 1 hr, and subsequent increases of the p52 protein levels (Figure 3B), indicating the activation of the noncanonical NF-κB pathway. However, we did not observe a reduction in the levels of IκBα by western blot, which is a hallmark of canonical NF-κB signaling activation (Figure 3B). The kinetics of viral RNA (vRNA) expression following the treatment of latently infected Jurkat cells with SBI-0637142 correlated with the observed induction of NIK-dependent NF-κB signaling (Figure S2B).

To determine whether the observed activation of HIV transcription by Smac mimetics is solely mediated through the NIK signaling axis, we generated a *NIK* knockout in the latently infected 2D10 cell line using a CRIPSR-based approach (Figure S2C). The loss of NIK abrogated the reactivation of latent HIV-1 through SBI-0637142 treatment, while not impinging upon the activity of PKC agonist bryostatin, an activator of canonical NF-κB signaling (Figure 3C). To further investigate the mechanism by which induction of the noncanonical pathway results in the LTR-dependent transcriptional activation of HIV-1, we have analyzed the nuclear translocation of NF-κB transcription factors upon treatment of CD4+ T cells with SBI-0637142 (Figure 3D). We found that both p52 and RELB translocate to the nucleus following BIRC2 depletion and NIK accumulation. In addition, low levels of RELA translocation were detected as well. Importantly, the translocation of RELA paralleled the delayed kinetics of NF-κB activation via the noncanonical NIK-p100 signaling axis, in contrast to the rapid nuclear accumulation resulting from TNFα stimulation. This suggests that activation of RELA was likely due to pathway crosstalk initiated after the induction of noncanonical signaling.

To further investigate this result, we used chromatin immunoprecipitation (ChIP) to assess the physical occupancy of the HIV-1 LTR by NF-κB transcription factors after induction of noncanonical signaling (Figure 3E). We find that Smac mimetic treatment leads to an association of RELB with the viral LTR, suggesting that noncanonical NF-κB transcription factors can

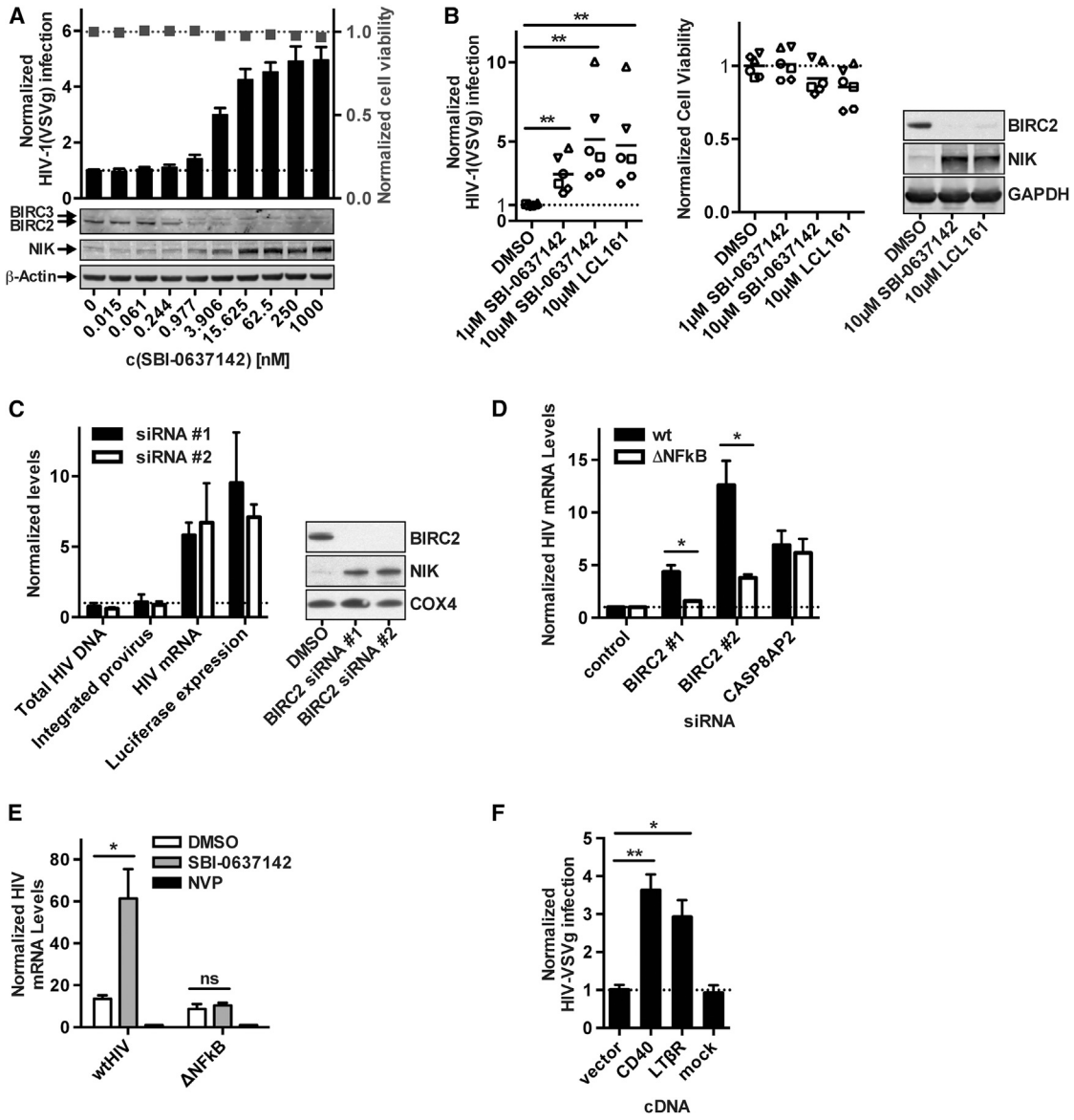

Figure 2. Effects of BIRC2 Depletion on HIV-1 Transcription in HEK293T Cells and Primary Cells

(A) HEK293T cells were treated with the BIRC2 antagonist SBI-0637142 at the indicated concentrations and infected with HIV-1(VSVg) for 24 hr. Levels of infection were evaluated by measuring luciferase reporter activity. Lysate of SBI-0637142-treated cells was evaluated for BIRC2 and NIK protein levels by western blot.

(B) Primary activated CD4+ T cells isolated from six healthy donors were treated with SBI-0637142 or LCL161 at the indicated concentrations for 24 hr. Cells were subsequently infected with HIV-1(VSVg) for 48 hr before analysis of luciferase reporter activity. Cell viability was evaluated by measuring cellular ATP levels. Each data point indicates mean of biological triplicates from a single donor. Lines indicate mean of six donors. BIRC2 depletion and NIK accumulation were analyzed by western blot.

(C) HIV-1(VSVg)-infected HEK293T cells treated with siRNAs targeting *BIRC2* were analyzed for levels of total HIV-1 DNA, integrated provirus, and HIV-1 mRNA by qPCR. Luciferase expression levels were evaluated in parallel. All values are normalized to nontargeting control siRNAs. BIRC2 and NIK protein expression levels upon siRNA treatment were analyzed by western blot.

(D) siRNA-treated HEK293T cells were infected with VSVg-pseudotyped HIV-1 (WT) or a virus mutant lacking functional NF-κB binding sites (ΔNFκB). Viral mRNA was measured by qPCR 24 hr after infection, and values were normalized to nontargeting control siRNAs. *CASP8AP2*-targeting siRNAs are shown as control.

(E) HEK293T cells were treated with 1 μM SBI-0637142 and infected for 24 hr with VSVg-pseudotyped HIV-1 containing either a functional or mutated NF-κB binding site in the viral LTR. HIV-1 mRNA levels were quantified by qPCR and normalized to samples from cells treated with 5 μM nevirapine (NVP).

(F) HEK293T cells transfected with vectors expressing CD40 or LTβR were subsequently infected with HIV-1(VSVg) for 24 hr. Viral infection was quantified by measuring expression of the viral encoded luciferase reporter and normalized to cells transfected with an empty vector as negative control.

All data are represented as mean ± SD of three biological replicates (A, B, and D) or as mean ± SEM of at least three independent experiments (E–G). p values were calculated using an unpaired t test with *$p < 0.05$ and **$p < 0.01$.

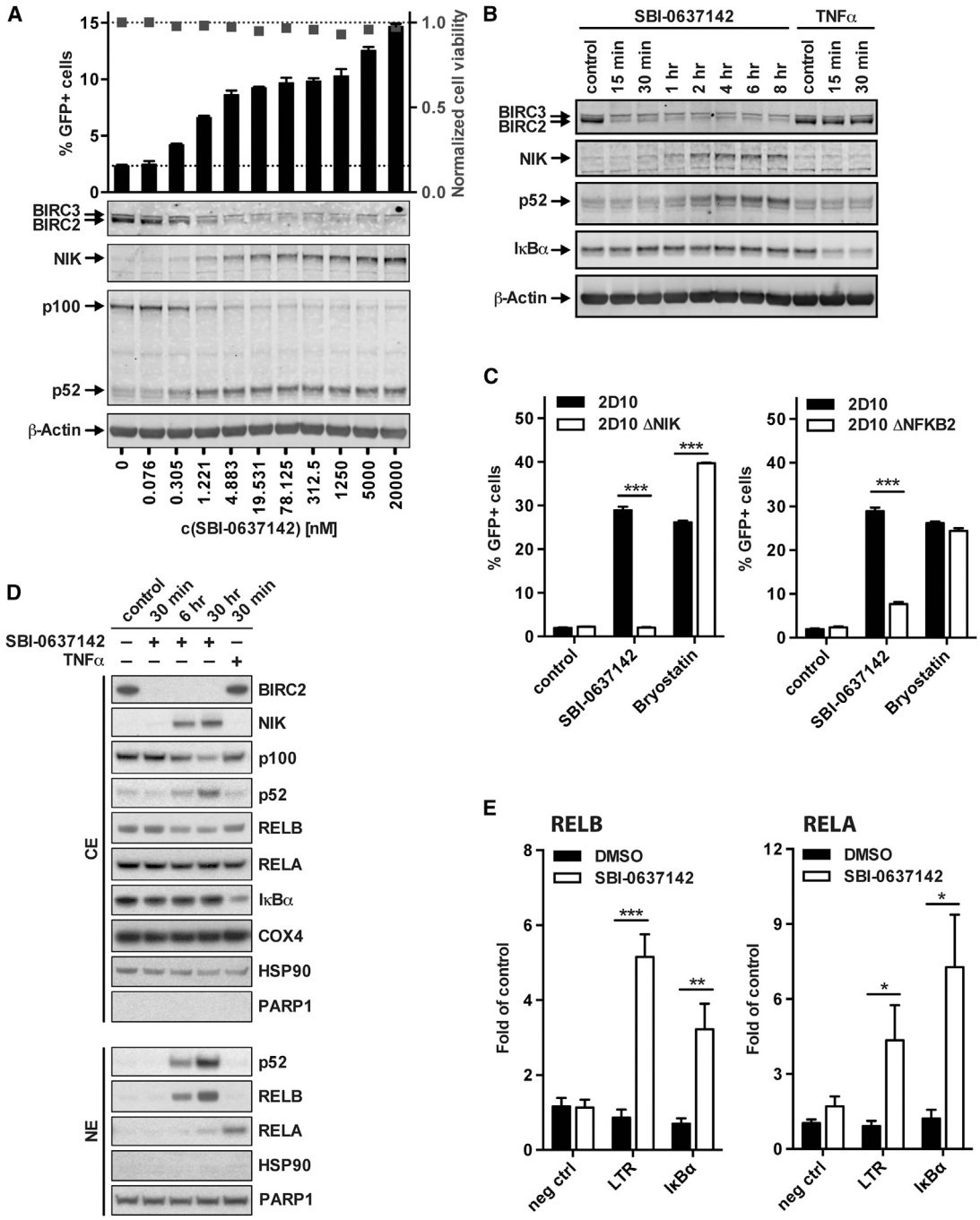

Figure 3. Smac Mimetic-Mediated BIRC2 Depletion Leads to the Reactivation of Latent HIV-1 in JLat Cells

(A) JLat 10.6 cells were treated with increasing amounts of SBI-0637142 for 36 hr. Reversal of latency was determined by FACS analysis of GPF expression. Depletion of BIRC2, accumulation of NIK, and processing of p100 to p52 were analyzed by western blot. FACS data are represented as mean ± SEM of three experiments.

(B) Kinetics of NF-κB activation upon treatment of JLat 10.6 cells with 1 μM SBI-0637142 were assessed by western blot. Treatment with 10 ng/ml TNFα served as positive control for canonical NF-κB pathway activation.

(C) 2D10 cells and clones with a knockout of *NIK* or *NFKB2* were incubated with 1 μM SBI-0637142 or 30 nM bryostatin for 36 hr. GFP expression was analyzed by FACS. Data are represented as mean ± SD of three biological replicates.

(D) CD4+ T cells from healthy donors were treated with 1 μM SBI-0637142 or 10 ng/ml TNFα. Cytoplasmic (CE) and nuclear (NE) extracts were analyzed by western blot. HSP90 and PARP1 served as control for cytoplasmic and nuclear proteins, respectively.

(E) 2D10 cells were treated with 1 μM SBI-0637142 for 9 hr prior to ChIP analysis using antibodies against RELA, RELB, or IgG as control. RELA- and RELB-specific association with the HIV-1 LTR and the IκBα gene promoter region, or an intergenic region upstream of the *PABPC1* gene not known to contain NF-κB binding sites as negative control, was analyzed by qPCR using specific primers and is shown as fold enrichment over IgG control. Data are represented as mean ± SEM of at least three experiments. *p < 0.05, **p < 0.01, ***p < 0.001, determined by unpaired t test.

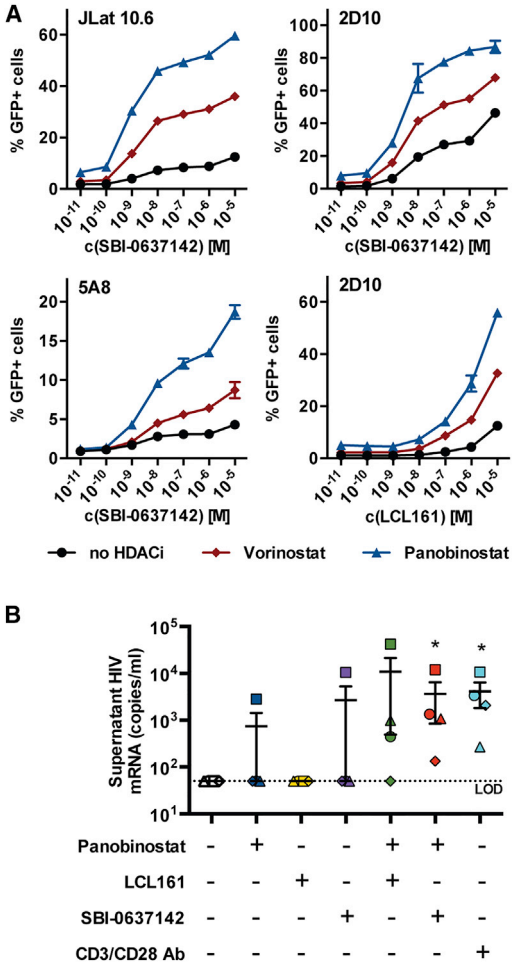

Figure 4. Combined Treatment with Smac Mimetics and HDAC Inhibitors Reverses HIV-1 Latency in Jurkat-Based Latency Models and Patient-Derived Resting CD4+ T Cells

(A) Latently infected Jurkat cell lines were treated with increasing amounts of SBI-0637142 alone or in combination with panobinostat or vorinostat. JLat 10.6 and 5A8 cells were treated with 10 nM panobinostat and 500 nM vorinostat, where indicated. 2D10 cells were treated with 5 nM panobinostat and 250 nM vorinostat. GFP expression was evaluated after 36 hr by FACS. Data are represented as mean ± SD of three biological replicates.

(B) Resting CD4+ T cells from HIV-1-infected patients under ART were treated with 100 nM panobinostat, 10 μM LCL161, 10 μM SBI-0637142, or a combination thereof for 48 hr. Viral production was subsequently evaluated by detection of viral mRNA in cell supernatants using qPCR. Data are represented as mean ± SEM of four donors. Significance of treatments was evaluated using a ratio paired t test. *$p < 0.05$.

directly influence HIV transcription. Moreover, we also detected binding of RELA to the HIV LTR, implicating a concerted action of both canonical and noncanonical transcription factors in HIV-1 activation upon Smac mimetic treatment. TNFα treatment, by contrast, resulted in RELA binding to the LTR but did not lead to a significant interaction with RELB (Figure S2D). To discern the functional contribution of the noncanonical RELB:p52 heterodimer to LRA activity after Smac mimetic treatment, we created a cell line with a knockout of the *NFKB2* gene, resulting in a loss of p100 expression (Figure S2E). In the absence of p100, and thereby p52, the reversal of HIV latency by Smac mimetics was reduced by ~75% (Figure 3C). Taken together, these results indicate that the LRA activity of Smac mimetics is solely initiated through the NIK-dependent noncanonical NF-κB signaling pathway. Induction of this pathway activates both the RELB:p52 heterodimer and, to a lesser extent, the RELA:p50 heterodimer, and results in the activation of LTR-dependent transcription that is primarily, but not exclusively, regulated by the noncanonical NF-κB transcription factor heterodimer.

BIRC2 Antagonist Treatment Acts Synergistically with HDAC Inhibitors to Reverse HIV-1 Latency

LRAs, such as PKC activators and HDAC inhibitors, have been shown to activate latent provirus synergistically (Burnett et al., 2010; Laird et al., 2015). We thus investigated the effects of Smac mimetics together with HDACis in three Jurkat-derived latency models—JLat 10.6, 2D10, and 5A8 cells (Figures 4A and S3A) (Pearson et al., 2008; Sakane et al., 2011). In each of the three cell lines tested, the combination of the Smac mimetic SBI-0637142, with either of the HDAC inhibitors panobinostat or vorinostat, reactivated latent provirus synergistically (Figure S3B). Although less potent, the Smac mimetic LCL161 showed similar synergy.

We next evaluated Smac mimetics for their ability to reverse latency in resting CD4+ T cells collected from HIV-1-infected patients undergoing ART (n = 4). Cells were treated with SBI-0637142 or LCL161 alone, or in combination with the HDACi panobinostat, and release of viral genomic RNA to the supernatant was measured by the recently described REVEAL (rapid ex vivo evaluation of antilatency) assay (Spivak et al., 2015). While none of the small molecules were found to activate latent provirus after 48 hr when used individually, both LCL161 and SBI-0637142 in combination with panobinostat were found to reactivate latent HIV-1 at levels comparable to those achieved upon treatment with antibodies against CD3 and CD28 (Figure 4B). Importantly, these results reach statistical significance ($p < 0.05$) for SBI-0637142 and CD3/CD28 antibody treatment, and no significant activation of resting CD4+ T cells was observed upon treatment with SBI-0637142 (Figure S3C).

DISCUSSION

Using a targeted siRNA screen, we identified *BIRC2*, a negative regulator of noncanonical NF-κB signaling, as a regulator of viral transcription. Critically, we observed that induction of noncanonical signaling results in both RELA:p50 and RELB:p52 heterodimeric transcription factors binding to the HIV-1 LTR, with genetic loss-of-function studies indicating that the transcriptional activation by RELB:p52 is the predominant regulator of this activity. Taken together, these results support an unappreciated role for the noncanonical NF-κB signaling machinery, and specifically RELB:p52, in the regulation of HIV-1 LTR-dependent transcription.

There have been considerable efforts focused on understanding the molecular basis of HIV-1 latency and devising pharmacological strategies to activate the latent provirus. Ideally, an LRA should only target cell types that are latently infected so as to avoid toxicity or widespread immune activation. In contrast to

strategies targeting canonical NF-κB signaling, it may be preferable to target components of the noncanonical NF-κB pathway, as it is active in a more restricted set of cell lineages. Smac mimetics are considered a promising new class of cancer therapeutics that are well tolerated in vivo, and primarily through their antagonism of XIAP, they promote apoptosis in tumor cells, while normal tissue remains unaffected (Fulda and Vucic, 2012). Many Smac mimetics can also trigger the noncanonical NF-κB signaling pathway through the depletion of BIRC2 or BIRC3. Although constitutive activation of the noncanonical NF-κB pathway through somatic mutations in mice has been associated with hematogenous malignancies including B cell lymphomas (Keats et al., 2007), proposed latency-reversing "shock and kill" approaches entail acute treatment regimens, largely mitigating these risks associated with chronic activation. In fact, six Smac mimetics, including LCL161, have been evaluated in clinical trials and have favorable safety and pharmacokinetic/pharmacodynamic (PK/PD) profiles (Bai et al., 2014). Unlike broadly acting Smac mimetics that target multiple proteins of the IAP family including the caspase inhibitor XIAP, certain compounds, such as SBI-0637142, preferentially target BIRC2 or BIRC3, the only known regulators of noncanonical NF-κB signaling among the IAP proteins (Finlay et al., 2014). Future studies will be required to investigate whether the observed increased potency of SBI-0637142 as an LRA may be related to its selectivity profile.

Many current strategies for reactivating latent HIV-1 focus on the use of PKC agonists to stimulate canonical NF-κB signaling. Due to toxicity risks, safety concerns have dampened enthusiasm for the use of these canonical NF-κB activators as LRAs (Morgan et al., 2012). HDACi have also shown promise as LRAs, with multiple compounds being evaluated in clinical trials (Rasmussen et al., 2013). Although HDACis increase intracellular levels of HIV-1 mRNA both in vitro and in vivo, the level of viral outgrowth induced by these compounds is likely insufficient to purge the viral reservoir (Bullen et al., 2014; Wei et al., 2014). Therefore, it is expected that a safe and effective drug regimen to reverse HIV-1 latency will require the combination of multiple agents (Xing and Siliciano, 2013), much like ART. Some HDACi have been shown to synergize with different classes of LRAs including PKC agonists (Laird et al., 2015), indicating that combinatorial use could increase efficacy while reducing required dosage. Consistently, we see similar levels of synergy between Smac mimetics and HDACi as levels reported for combinatorial treatment with HDACi and PKC agonists (Wong et al., 2014).

Given the scarcity of clinical data to date, the optimal strategy for reversing HIV-1 latency in patients is far from certain. Our results demonstrating that Smac mimetics, in conjunction with the HDACi panobinostat, can reverse latency in patient-derived resting CD4+ T cells suggest a promising clinical approach toward the development of a "cure" for patients with HIV-1. Importantly, the established clinical safety and pharmacodynamic profiles of Smac mimetics should enable this class of small molecule antagonists to be readily evaluated as a therapeutic strategy. Taken together, these data indicate that rapid preclinical development and clinical repositioning of Smac mimetics may help provide a safe and effective combinatorial therapeutic regimen to eradicate HIV-1.

EXPERIMENTAL PROCEDURES

siRNA Transfections and Infection with HIV-1

siRNA transfections of HEK293T cells and infections with a single-cycle envelope deleted, VSV-G-pseudotyped HIV-1 reporter virus (HIV-1[VSVg]), were performed as previously described (König et al., 2008). Cells were infected 48 hr after siRNA transfection, and luciferase expression levels were determined 24 hr after infection. Mapping to viral replication cycle stages was done by isolating mRNA and DNA from infected cells and quantifying proviral DNA content, total HIV DNA, and HIV mRNA levels by qPCR. Cells infected with VSV-G-pseudotyped HIV-1 containing either wild-type or mutant NF-κB binding sites in the LTR (Bosque and Planelles, 2009) were analyzed by measuring HIV mRNA levels by qPCR. Cell viability was analyzed using the ATPlite cell viability assay (Perkin Elmer).

HIV-1 Infection of Human CD4+ T Cells

Following isolation, CD4+ T cells from healthy donors were activated with 4 μg/ml phytohemagglutinin-P (PHA, Sigma) for 48 hr. Activated CD4+ T cells were treated with compounds for 24 hr prior to infection with HIV-1(VSVg). Luciferase expression levels were normalized to mock-treated cells; mean of DMSO-treated cells was defined as 1.

Jurkat HIV Latency Model

Latently infected Jurkat cells were treated with compounds and subsequently analyzed for GFP expression by flow cytometry. Analytical cytometry was performed in the Sanford Burnham Prebys Flow Cytometry Core. Cell viability was determined using the ATPlite cell viability assay.

Chromatin Immunoprecipitation

2D10 cells were stimulated with 1 μM SBI-0637142 or DMSO for 9 hr prior to ChIP using antibodies targeting RELA and RELB.

Treatment of Resting CD4+ T Cells from Aviremic HIV Patients

Resting CD4+ T cells isolated from aviremic HIV-1-infected patients on ART were cultured in the presence or absence of reactivating compounds for 48 hr. Culture supernatants were analyzed by two-step qPCR using a primer and probe set for conserved regions of the 3′ LTR of HIV-1 mRNA as previously described (Spivak et al., 2015).

Please refer to the Supplemental Experimental Procedures for additional information.

SUPPLEMENTAL INFORMATION

Supplemental Information includes three figures, two tables, and Supplemental Experimental Procedures and can be found with this article at http://dx.doi.org/10.1016/j.chom.2015.08.009.

AUTHOR CONTRIBUTIONS

L.P., J.A.T.Y., and S.K.C. conceived the study. L.P., J.M.M., Y.H., A.M.M., L.M., and R.K. conducted screening and validation experiments. L.P., M.S.D., and J.P.M. conducted mechanistic studies. A.M.S., L.J.M., and A.B. conducted patient cell assays. M.V., P.T., and N.D.P.C. developed and synthesized compounds. V.S., A.F.-S., N.D.P.C., F.D.B., J.A.T.Y., V.P., and S.K.C. supervised the studies. L.P. and S.K.C. wrote the manuscript.

ACKNOWLEDGMENTS

We are grateful for advice on flow cytometry from D. Chambers and C. O'Connor (Salk Institute) and for assistance with viral stock preparation from The Salk Institute Gene Transfer, Targeting, and Therapeutics Core. We thank Carl Ware (Sanford Burnham Prebys Medical Discovery Institute) for providing cDNA constructs of NF-κB regulators. We would like to thank Warner C. Greene (Gladstone Institutes) for making the cell line 5A8 available to us. We thank Jonathan Karn (Case Western Reserve University) for providing the cell line 2D10. This study was supported by NIH/NIAID grants P01 AI090935 to A.F.-S., V.S., F.D.B., J.A.T.Y., and S.K.C.; by grant R01 DA033773 to S.K.C.; and by grant R01 AI087508 to V.P. We acknowledge funding from

NIH/NIAID grants 5R01 AI073450 and HHSN272201400008C and from DOD/DARPA grant HR0011-11-C-0094 to A.F.-S. This work was also supported by a generous grant from the James B. Pendleton Charitable Trust to support HIV/AIDS research. J.P.M. is currently an employee of Gilead Sciences. J.A.T.Y. is currently employed by F. Hoffmann-La Roche Ltd. All contributions by J.P.M. and J.A.T.Y. to this study occurred prior to their employment at Gilead Sciences and F. Hoffmann-La Roche Ltd., respectively.

Received: April 2, 2015
Revised: July 22, 2015
Accepted: August 25, 2015
Published: September 9, 2015

REFERENCES

Agarwal, S., Harada, J., Schreifels, J., Lech, P., Nikolai, B., Yamaguchi, T., Chanda, S.K., and Somia, N.V. (2006). Isolation, characterization, and genetic complementation of a cellular mutant resistant to retroviral infection. Proc. Natl. Acad. Sci. USA *103*, 15933–15938.

Bai, L., Smith, D.C., and Wang, S. (2014). Small-molecule SMAC mimetics as new cancer therapeutics. Pharmacol. Ther. *144*, 82–95.

Basak, S., Kim, H., Kearns, J.D., Tergaonkar, V., O'Dea, E., Werner, S.L., Benedict, C.A., Ware, C.F., Ghosh, G., Verma, I.M., and Hoffmann, A. (2007). A fourth IkappaB protein within the NF-kappaB signaling module. Cell *128*, 369–381.

Bosque, A., and Planelles, V. (2009). Induction of HIV-1 latency and reactivation in primary memory CD4+ T cells. Blood *113*, 58–65.

Britanova, L.V., Makeev, V.J., and Kuprash, D.V. (2008). In vitro selection of optimal RelB/p52 DNA-binding motifs. Biochem. Biophys. Res. Commun. *365*, 583–588.

Bullen, C.K., Laird, G.M., Durand, C.M., Siliciano, J.D., and Siliciano, R.F. (2014). New ex vivo approaches distinguish effective and ineffective single agents for reversing HIV-1 latency in vivo. Nat. Med. *20*, 425–429.

Burnett, J.C., Lim, K.I., Calafi, A., Rossi, J.J., Schaffer, D.V., and Arkin, A.P. (2010). Combinatorial latency reactivation for HIV-1 subtypes and variants. J. Virol. *84*, 5958–5974.

Donahue, D.A., and Wainberg, M.A. (2013). Cellular and molecular mechanisms involved in the establishment of HIV-1 latency. Retrovirology *10*, 11.

Finlay, D., Vamos, M., González-López, M., Ardecky, R.J., Ganji, S.R., Yuan, H., Su, Y., Cooley, T.R., Hauser, C.T., Welsh, K., et al. (2014). Small-molecule IAP antagonists sensitize cancer cells to TRAIL-induced apoptosis: roles of XIAP and cIAPs. Mol. Cancer Ther. *13*, 5–15.

Fulda, S., and Vucic, D. (2012). Targeting IAP proteins for therapeutic intervention in cancer. Nat. Rev. Drug Discov. *11*, 109–124.

Fusco, A.J., Huang, D.B., Miller, D., Wang, V.Y., Vu, D., and Ghosh, G. (2009). NF-kappaB p52:RelB heterodimer recognizes two classes of kappaB sites with two distinct modes. EMBO Rep. *10*, 152–159.

Groschel, B., and Bushman, F. (2005). Cell cycle arrest in G2/M promotes early steps of infection by human immunodeficiency virus. J. Virol. *79*, 5695–5704.

Gummuluru, S., and Emerman, M. (1999). Cell cycle- and Vpr-mediated regulation of human immunodeficiency virus type 1 expression in primary and transformed T-cell lines. J. Virol. *73*, 5422–5430.

Infante, J.R., Dees, E.C., Olszanski, A.J., Dhuria, S.V., Sen, S., Cameron, S., and Cohen, R.B. (2014). Phase I dose-escalation study of LCL161, an oral inhibitor of apoptosis proteins inhibitor, in patients with advanced solid tumors. J. Clin. Oncol. *32*, 3103–3110.

Keats, J.J., Fonseca, R., Chesi, M., Schop, R., Baker, A., Chng, W.J., Van Wier, S., Tiedemann, R., Shi, C.X., Sebag, M., et al. (2007). Promiscuous mutations activate the noncanonical NF-kappaB pathway in multiple myeloma. Cancer Cell *12*, 131–144.

König, R., Zhou, Y., Elleder, D., Diamond, T.L., Bonamy, G.M., Irelan, J.T., Chiang, C.Y., Tu, B.P., De Jesus, P.D., Lilley, C.E., et al. (2008). Global analysis of host-pathogen interactions that regulate early-stage HIV-1 replication. Cell *135*, 49–60.

Laird, G.M., Bullen, C.K., Rosenbloom, D.I., Martin, A.R., Hill, A.L., Durand, C.M., Siliciano, J.D., and Siliciano, R.F. (2015). Ex vivo analysis identifies effective HIV-1 latency-reversing drug combinations. J. Clin. Invest. *125*, 1901–1912.

Manganaro, L., Pache, L., Herrmann, T., Marlett, J., Hwang, Y., Murry, J., Miorin, L., Ting, A.T., König, R., García-Sastre, A., et al. (2014). Tumor suppressor cylindromatosis (CYLD) controls HIV transcription in an NF-κB-dependent manner. J. Virol. *88*, 7528–7540.

Margolis, D.M. (2010). Mechanisms of HIV latency: an emerging picture of complexity. Curr. HIV/AIDS Rep. *7*, 37–43.

Margolis, D.M. (2011). Histone deacetylase inhibitors and HIV latency. Curr. Opin. HIV AIDS *6*, 25–29.

Morgan, R.J., Jr., Leong, L., Chow, W., Gandara, D., Frankel, P., Garcia, A., Lenz, H.J., and Doroshow, J.H. (2012). Phase II trial of bryostatin-1 in combination with cisplatin in patients with recurrent or persistent epithelial ovarian cancer: a California cancer consortium study. Invest. New Drugs *30*, 723–728.

Nabel, G., and Baltimore, D. (1987). An inducible transcription factor activates expression of human immunodeficiency virus in T cells. Nature *326*, 711–713.

Nguyen, D.G., Yin, H., Zhou, Y., Wolff, K.C., Kuhen, K.L., and Caldwell, J.S. (2007). Identification of novel therapeutic targets for HIV infection through functional genomic cDNA screening. Virology *362*, 16–25.

Pearson, R., Kim, Y.K., Hokello, J., Lassen, K., Friedman, J., Tyagi, M., and Karn, J. (2008). Epigenetic silencing of human immunodeficiency virus (HIV) transcription by formation of restrictive chromatin structures at the viral long terminal repeat drives the progressive entry of HIV into latency. J. Virol. *82*, 12291–12303.

Rasmussen, T.A., Tolstrup, M., Winckelmann, A., Østergaard, L., and Søgaard, O.S. (2013). Eliminating the latent HIV reservoir by reactivation strategies: advancing to clinical trials. Hum. Vaccin. Immunother. *9*, 790–799.

Sakane, N., Kwon, H.S., Pagans, S., Kaehlcke, K., Mizusawa, Y., Kamada, M., Lassen, K.G., Chan, J., Greene, W.C., Schnoelzer, M., and Ott, M. (2011). Activation of HIV transcription by the viral Tat protein requires a demethylation step mediated by lysine-specific demethylase 1 (LSD1/KDM1). PLoS Pathog. *7*, e1002184.

Shih, V.F., Tsui, R., Caldwell, A., and Hoffmann, A. (2011). A single NFκB system for both canonical and non-canonical signaling. Cell Res. *21*, 86–102.

Spivak, A.M., Bosque, A., Balch, A.H., Smyth, D., Martins, L., and Planelles, V. (2015). Ex Vivo Bioactivity and HIV-1 Latency Reversal by Ingenol Dibenzoate and Panobinostat in Resting CD4+ T Cells from Aviremic Patients. Antimicrob. Agents Chemother. http://dx.doi.org/10.1128/AAC.01077-15, AAC.01077-15.

Sun, S.C. (2012). The noncanonical NF-κB pathway. Immunol. Rev. *246*, 125–140.

Vamos, M., Welsh, K., Finlay, D., Lee, P.S., Mace, P.D., Snipas, S.J., Gonzalez, M.L., Ganji, S.R., Ardecky, R.J., Riedl, S.J., et al. (2013). Expedient synthesis of highly potent antagonists of inhibitor of apoptosis proteins (IAPs) with unique selectivity for ML-IAP. ACS Chem. Biol. *8*, 725–732.

Wei, D.G., Chiang, V., Fyne, E., Balakrishnan, M., Barnes, T., Graupe, M., Hesselgesser, J., Irrinki, A., Murry, J.P., Stepan, G., et al. (2014). Histone deacetylase inhibitor romidepsin induces HIV expression in CD4 T cells from patients on suppressive antiretroviral therapy at concentrations achieved by clinical dosing. PLoS Pathog. *10*, e1004071.

Williams, S.A., Chen, L.F., Kwon, H., Ruiz-Jarabo, C.M., Verdin, E., and Greene, W.C. (2006). NF-kappaB p50 promotes HIV latency through HDAC recruitment and repression of transcriptional initiation. EMBO J. *25*, 139–149.

Wong, V.C., Fong, L.E., Adams, N.M., Xue, Q., Dey, S.S., and Miller-Jensen, K. (2014). Quantitative evaluation and optimization of co-drugging to improve anti-HIV latency therapy. Cell. Mol. Bioeng. *7*, 320–333.

Xing, S., and Siliciano, R.F. (2013). Targeting HIV latency: pharmacologic strategies toward eradication. Drug Discov. Today *18*, 541–551.

Zarnegar, B.J., Wang, Y., Mahoney, D.J., Dempsey, P.W., Cheung, H.H., He, J., Shiba, T., Yang, X., Yeh, W.C., Mak, T.W., et al. (2008). Noncanonical NF-kappaB activation requires coordinated assembly of a regulatory complex of the adaptors cIAP1, cIAP2, TRAF2 and TRAF3 and the kinase NIK. Nat. Immunol. *9*, 1371–1378.

Cell Host & Microbe, Volume *18*

Supplemental Information

BIRC2/cIAP1 Is a Negative Regulator of HIV-1 Transcription and Can Be Targeted by Smac Mimetics to Promote Reversal of Viral Latency

Lars Pache, Miriam S. Dutra, Adam M. Spivak, John M. Marlett, Jeffrey P. Murry, Young Hwang, Ana M. Maestre, Lara Manganaro, Mitchell Vamos, Peter Teriete, Laura J. Martins, Renate König, Viviana Simon, Alberto Bosque, Ana Fernandez-Sesma, Nicholas D.P. Cosford, Frederic D. Bushman, John A.T. Young, Vicente Planelles, and Sumit K. Chanda

A

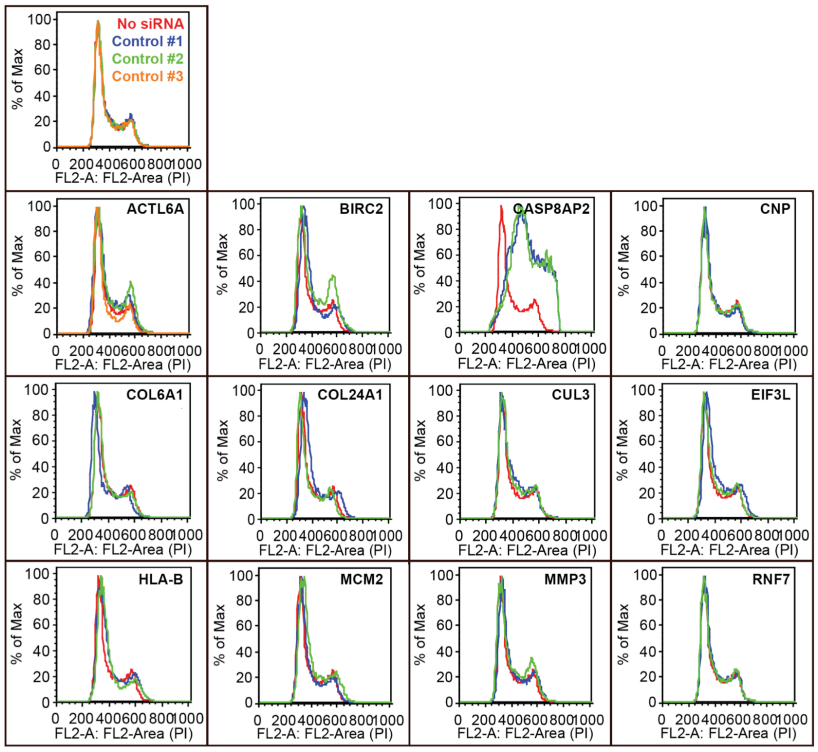
No siRNA
Control #1
Control #2
Control #3
% of Max
FL2-A: FL2-Area (PI)
ACTL6A
BIRC2
CASP8AP2
CNP
COL6A1
COL24A1
CUL3
EIF3L
HLA-B
MCM2
MMP3
RNF7

B

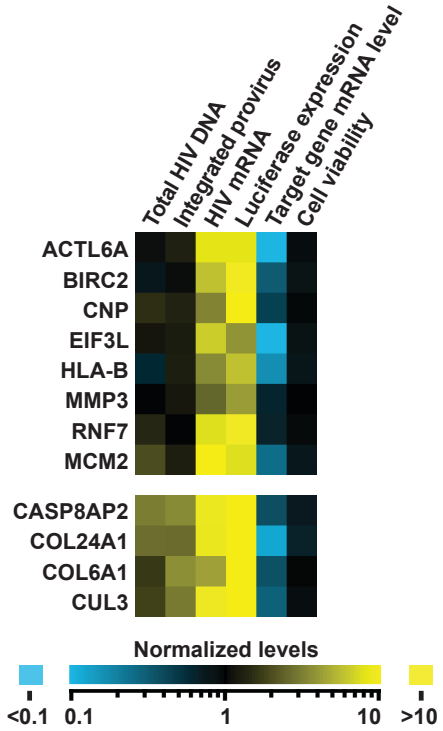
Total HIV DNA
Integrated provirus
HIV mRNA
Luciferase expression
Target gene mRNA level
Cell viability
ACTL6A
BIRC2
CNP
EIF3L
HLA-B
MMP3
RNF7
MCM2
CASP8AP2
COL24A1
COL6A1
CUL3
Normalized levels
<0.1
0.1
1
10
>10

Figure S1

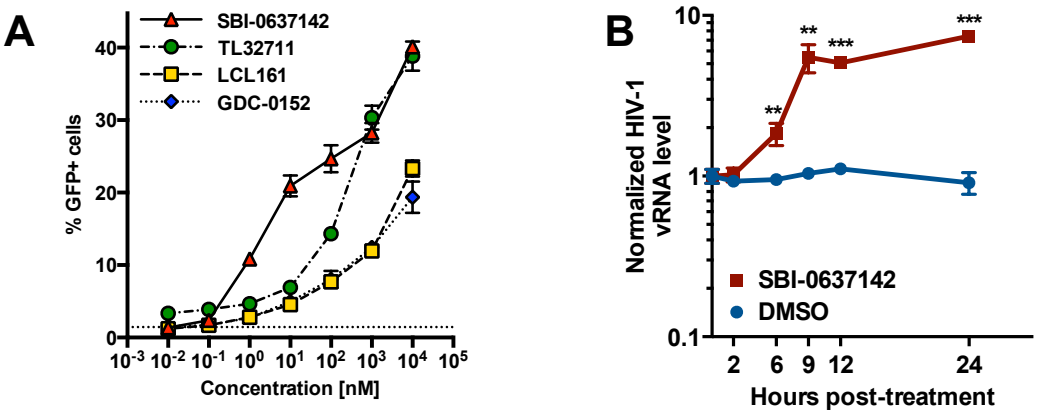
A
SBI-0637142
TL32711
LCL161
GDC-0152
% GFP+ cells
Concentration [nM]
B
Normalized HIV-1 vRNA level
SBI-0637142
DMSO
Hours post-treatment

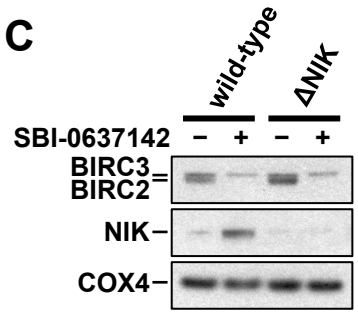
C
wild-type
ΔNIK
SBI-0637142
BIRC3
BIRC2
NIK
COX4

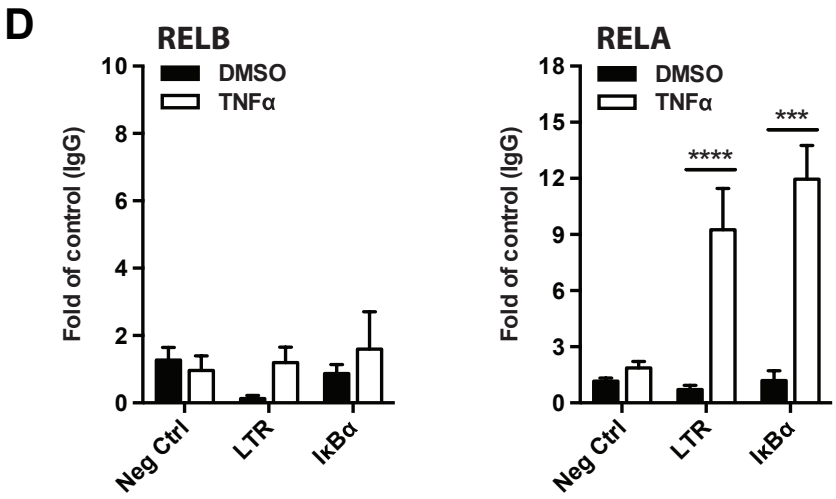
D
RELB
RELA
DMSO
TNFα
Fold of control (IgG)
Neg Ctrl
LTR
IκBα

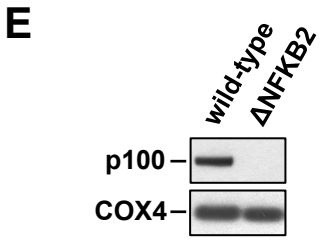
E
wild-type
ΔNFKB2
p100
COX4

Figure S2

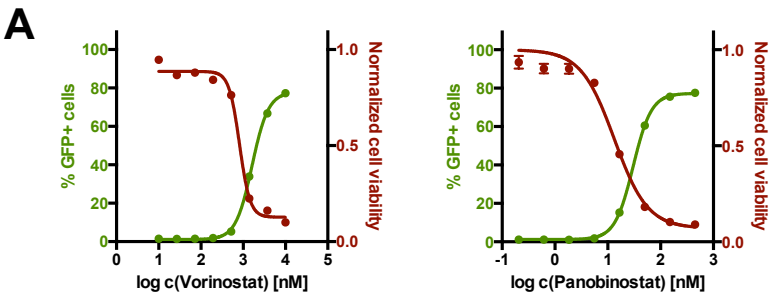
A
% GFP+ cells
Normalized cell viability
log c(Vorinostat) [nM]
log c(Panobinostat) [nM]

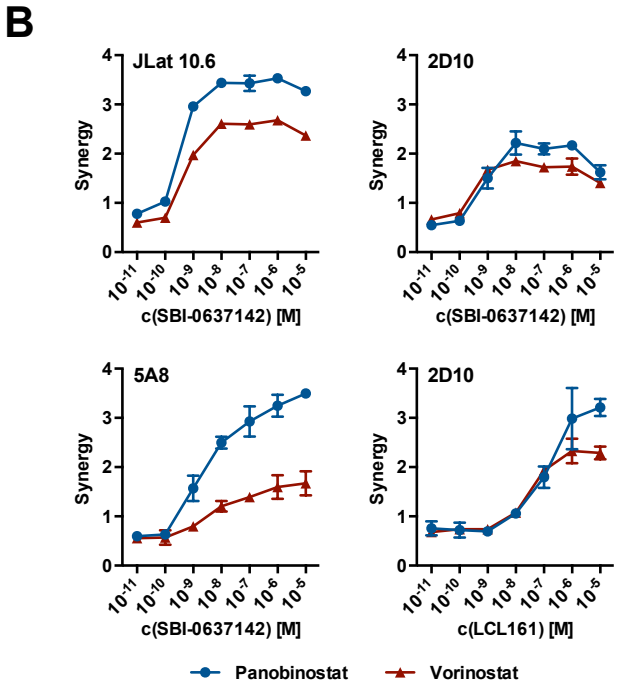
B
JLat 10.6
2D10
5A8
2D10
Synergy
c(SBI-0637142) [M]
c(LCL161) [M]
Panobinostat
Vorinostat

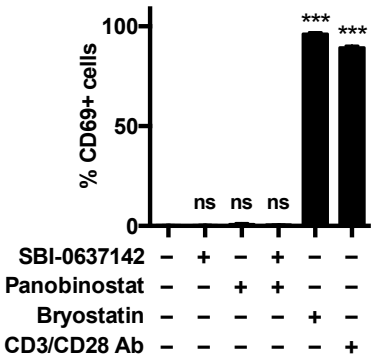
C
% CD69+ cells
ns
***
SBI-0637142
Panobinostat
Bryostatin
CD3/CD28 Ab

Figure S3

SUPPLEMENTAL FIGURE LEGENDS

Figure S1, related to Figure 1.

(A) Analysis of cell cycle progression upon gene knockdown. Cell cycle progression of HEK293T cells treated with individual siRNAs was evaluated by staining of the cells with propidium iodide and subsequent analysis by FACS. Transfection with non-targeting siRNAs (controls) was compared to untransfected cells. Non-targeting control siRNA #1 (red) and 2 or 3 targeting siRNAs (green, blue, orange) are shown for each indicated gene.

(B) Heatmap showing the effects of identified genes on specific steps of HIV-1 replication. HEK293T cells were treated with individual siRNAs targeting the indicated genes. Following infection with HIV-1(VSVg) the levels of HIV-1 total DNA, integrated provirus, and HIV-1 mRNA were determined by qPCR. Also shown are luciferase expression levels, target gene knockdown levels, and cell viability upon target gene knockdown. All values are normalized to non-targeting control siRNAs.

Figure S2, related to Figure 3.

(A) Smac mimetics act as latency reversing agents. 2D10 cells were treated with SBI-0637142, TL32711 (Birinapant), LCL161, or GDC-0152 for 36 hours at the indicated concentrations. Reversal of HIV latency was evaluated by measuring GFP expression using flow cytometry. Data are represented as mean ± SD of three biological replicates. Dotted line represents values of untreated cells.

(B) Kinetics of viral RNA expression in latently infected Jurkat cells upon Smac mimetic treatment. 2D10 cells were treated with 1μM SBI-0637142 or DMSO as negative control. Intracellular viral RNA levels were determined by qPCR at the time points indicated. Data was normalized to GAPDH. Graph shows mean ± SD of three biological replicates. ** indicates $p < 0.01$, *** indicates $p < 0.001$, determined by unpaired t-test.

(C) Knockout of *NIK* in 2D10 cells. Wild-type 2D10 cells and a clone with a knockout of *NIK* were treated with DMSO or 1μM SBI-0637142 and analyzed by Western blot for NIK expression levels.

(D) Impact of TNFα treatment on RELA and RELB interaction with the HIV-1 LTR. 2D10 cells were treated with 20ng/ml TNFα for 2 hours prior to ChIP analysis using antibodies against RELA, RELB, or IgG as control. RELA and RELB specific association with the HIV-1 LTR and the IκBα gene promoter region, or an intergenic region upstream of the *PABPC1* gene unknown to contain NF-κB binding sites as negative control, was detected by qPCR using specific primers and is shown as fold enrichment over IgG control. Data are represented as mean ± SEM of at least three experiments. *** indicates $p \leq 0.001$, **** indicates $p \leq 0.0001$, determined by unpaired t-test.

(E) Knockout of *NFKB2* in 2D10 cells. Wild-type 2D10 cells and a clone with a knockout of *NFKB2* were analyzed by Western blot for p100 expression levels.

Figure S3, related to Figure 4.

(A) Dose response of JLat 10.6 cells treated with HDACi. Following treatment with panobinostat or vorinostat for 36 hours JLat 10.6 cells were evaluated for reactivation of latent provirus by measuring GFP expression using flow cytometry. Cell viability was assessed by determining cellular ATP levels.

(B) Level of drug synergy between Smac mimetic and HDACi. The level of synergy between HDACi and Smac mimetics, when used in combination (see Fig. 4A), was evaluated using the Bliss independence model. Data are represented as mean ± SD of biological triplicates.

(C) Activation of resting CD4+ T cells upon LRA treatment. Resting CD4+ T cells from three healthy donors were treated with 10μM SBI-0637142, 100nM Panobinostat, 30nM Bryostatin, CD3/CD28 antibody beads, or a combination thereof, for 48 hours prior to analysis of CD69 surface expression by FACS. Data is represented as mean ± SEM of three donors. *** indicates $p < 0.001$ determined by unpaired t-test.

Table S1, related to Figure 1B:
139 genes identified by siRNA screen in HIV-1(VSVg)-infected HIK293T cells.

Gene symbol	Normalized luciferase activity [fold change] - siRNA A	Normalized luciferase activity [fold change] - siRNA B
CYLD	16.4357	8.0944
BAF53A	10.1565	7.0609
MCM2	9.7744	4.0175
RNF7	5.8401	4.9686
DCLRE1C	12.3409	2.2605
CASP8AP2	5.7124	4.5880
SPTAN1	10.7234	2.3932
PPP2CA	8.8763	2.6937
MMP3	5.3252	4.1427
CNP	5.3847	3.7683
BCL2	12.6254	1.5834
SEC3L1	9.9753	1.8056
NFKBIA	9.9132	1.7373
PCNA	4.1222	3.8537
ABCG1	5.7841	2.6632
SOM	5.9403	2.3594
BIRC2	4.1112	3.3360
KIAA0648	4.9677	2.6731
TNFRSF1B	4.1992	3.0572
USP46	3.8782	3.2180
BAT4	3.7861	3.0525
CUL3	5.0121	2.0836
POLA	3.7217	2.7096
SST	3.3463	2.9389
MARK2	3.9664	2.3973
PHTF2	4.8546	1.8507
COL6A1	3.1367	2.8366
MAPK10	3.5729	2.4794
CREB1	5.3028	1.5919
COL24A1	2.9147	2.8661
CDC2	3.1238	2.6416
CXCL13	3.5870	2.1635
RNPS1	3.7430	2.0510
UBE2A	3.5199	2.1686
APOC2	3.9817	1.8456
RPA1	2.9917	2.4401
IGSF9	3.0338	2.3950
ASC	4.8232	1.5042
H1FX	3.1979	2.2524
ARF1	3.0811	2.2672
LOC147991	2.9412	2.3601
GNB2L1	2.6431	2.5699
NEUROG3	2.6075	2.5936
KIAA0543	3.0436	2.1472
SMAP-1	4.0219	1.6200
RRM2	3.1676	2.0481
COPG	2.8100	2.2975
MOV10	2.7541	2.3392
FLJ34389	3.9919	1.5913
INCENP	3.4727	1.7849
DDIT4L	3.3447	1.8339
DSP	3.0084	2.0064
SPG7	2.5784	2.3379
HB-1	3.1201	1.8974
TMED2	3.0156	1.9556
TRIP	3.1244	1.8852
WNT9B	2.7210	2.1483
APLP1	3.3806	1.6463
CALR	2.6426	2.1059
LOC124245	2.8733	1.9365
BYSL	2.5379	2.1728
TOLLIP	2.9194	1.8134
SARDH	2.5755	2.0454
NUDT3	2.7249	1.9146
SKP1A	2.6008	1.9888

HUWE1	2.5555	2.0209
HIST1H2BG	3.1588	1.6244
RPS28	2.8781	1.7753
PTP4A1	2.2823	2.2267
LOC56902	2.6710	1.8952
ARL6IP	2.2796	2.2148
WWP1	3.1838	1.5402
FOXF1	2.2049	2.2021
FLJ10652	2.2817	2.1052
TRAF3	2.5508	1.8490
HNRPD	1.9816	2.3622
PCDHGC5	2.4096	1.9204
FKBP9	2.7999	1.6354
GFPT1	2.8429	1.5990
FYN	2.2625	1.9757
RFC3	2.4740	1.7898
RPS19	2.4816	1.7757
TCEB1	2.0571	2.1322
COL25A1	2.2629	1.9360
ARL10B	2.1091	2.0735
N4BP2	2.3102	1.8737
ARID5A	2.6680	1.6122
ELAVL1	2.4303	1.7147
PSIP1	2.3450	1.7684
A1BG	2.4770	1.6692
FBXO39	2.4382	1.6781
C10ORF58	2.2061	1.8450
HLA-B	2.2398	1.8131
MRE11A	2.4244	1.6656
MAPK6	2.3082	1.7492
CUL2	2.5064	1.5954
DUSP6	2.0443	1.9428
NFIB	2.1595	1.8185
RRM1	2.0690	1.8970
CUTL1	1.9807	1.9483
LRRC4B	1.9675	1.9338
VSNL1	2.2678	1.6776
CUL1	2.4034	1.5814
SMOC2	2.2119	1.7071
TMEM42	2.2623	1.6625
VCP	2.0463	1.8119
CIRBP	1.9906	1.8221
CAMK2G	2.0364	1.7797
LOC155054	2.0052	1.7965
RNF31	2.2811	1.5740
PDGFA	1.8798	1.8720
UGT2A1	2.0627	1.6740
TUSC2	2.1243	1.6231
CDT1	1.9329	1.7759
TBCD	1.8974	1.7942
OGT	2.0277	1.6737
SMARCB1	2.1654	1.5227
BIRC5	1.8156	1.8095
XPO1	1.8288	1.7945
NUDT10	1.9933	1.6150
FLJ20512	1.9537	1.5846
MUS81	1.7882	1.7270
GOLPH3	1.8379	1.6636
FLJ38984	1.8912	1.5810
BG1	1.7766	1.6733
RLN2	1.7620	1.6737
WNT9A	1.7755	1.6558
EIF3L	1.8948	1.5380
ZDHHC8	1.7427	1.6609
HIST1H1C	1.8701	1.5416
REPS1	1.7222	1.6691
RFP2	1.7119	1.6743
ZNF142	1.7932	1.5650
GMDS	1.8369	1.5154
LOC90693	1.7829	1.5568
UBE2L3	1.6680	1.6261
PASK	1.7468	1.5258
MEGF11	1.6399	1.6026
DNCLI1	1.7097	1.5180

Table S2, related to Figure 1D: Results of validated siRNAs in HIV-1(VSVg) infection assay

Entrez Gene ID	NCBI Gene Symbol	siRNA used for life cycle mapping	siRNA target sequence	Normalized luciferase expression [fold increase]	Normalized cell viability [%]	Normalized target gene expression level [%]
86	ACTL6A	*	AAAGCTTTAACTGGCTCTATA	8.1	92.2	7.0
86	ACTL6A		CACAATGTTAGGAGTCAGTCA	8.1	67.4	17.3
329	BIRC2	*	TCCCAGGTCCCTCGTATCAAA	9.5	84.1	31.7
329	BIRC2		CTAGGAGACAGTCCTATTCAA	7.1	71.2	39.3
9994	CASP8AP2		CAGCTGATGTGCGGAAGTCAA	10.8	70.9	37.5
9994	CASP8AP2	*	CAGTCTGATCTCAATAAGGAA	21.4	73.0	37.3
1267	CNP		CAGGGCCTTGCTAATCGGGTT	11.9	104.2	48.6
1267	CNP	*	CGCCGGGACATCAGAATTCTT	11.3	95.7	43.7
255631	COL24A1		AACACTCTACTTGAACCTAAA	4.5	80.1	33.5
255631	COL24A1	*	CTGAACTACCTTAGCAATTTA	14.9	65.4	11.9
1291	COL6A1		CACCATCGTGGACATGATCAA	10.3	87.8	22.3
1291	COL6A1	*	CCCGGGTTTGACGGCATTCAA	11.3	102.2	36.4
8452	CUL3		AACAACTTTCTTCAAACGCTA	26.3	77.1	37.5
8452	CUL3	*	TCGAGATCAAGTTGTACGTTA	41.2	90.7	29.3
51386	EIF3L	*	TACGCTTATCCCAGCGACTAT	3.8	86.8	7.9
51386	EIF3L		AAGCGAGGCAGCCATGTCTTA	2.6	92.2	10.8
3106	HLA-B	*	TCCTGGAATTTGAGAGAGCAA	5.8	78.8	16.4
3106	HLA-B		CGGGCATGACCAGTACGCCTA	4.0	91.7	15.8
4171	MCM2	*	CTGCGGGACTATGTGATCGAA	7.6	76.6	25.4
4171	MCM2		CTCATTGGAGATGGCATGGAA	4.7	89.5	13.0
4314	MMP3	*	AGGGATTGACTCAAAGATTGA	4.1	98.8	62.1
4314	MMP3		GACAGTGGTCCTGTTGTTAAA	2.9	96.6	39.7
9616	RNF7	*	CTGTTCAATCATTGAGTGGTA	9.3	94.3	64.9
9616	RNF7		ATGCTTATGGTTGATCAGTTA	7.3	80.0	42.5

SUPPLEMENTAL EXPERIMENTAL PROCEDURES

siRNA transfections. Individual siRNAs were transfected into HEK293T cells at a concentration of 12.5 nM using RNAiMAX Transfection Reagent (Life Technologies) following a reverse transfection protocol as previously described (König et al., 2007). Cells were infected with HIV-1(VSVg) 48 hours post transfection (König et al., 2008).

Viral infections with luciferase reporter virus. VSV-G-pseudotyped lentiviral supernatant (HIV-1(VSVg)) was generated using the pNL43-Luc-E-R+ (HIV-1 wild-type Δenv, encoding firefly luciferase GL3) vector as previously described (König et al., 2007). Following a 24 hour incubation of cells with HIV-1(VSVg), luciferase expression levels were determined using the Bright-Glo Luciferase Assay System (Perkin Elmer). A second set of siRNA-transfected cells was mock infected and cell viability was determined 72 hours post transfection using the ATPlite cell viability assay (Perkin Elmer).

Infection with LTR mutant viruses. HEK293T cells transfected with siRNA or treated with compounds were infected with VSV-G-pseudotyped HIV-1 containing either wild-type or mutant NF-κB binding sites in the LTR (Bosque and Planelles, 2009). After 24 hours of infection HIV-1 mRNA levels were analyzed by qPCR as described below.

Mapping to viral life cycle stages. HEK293T cells were transfected with individual siRNAs and infected with HIV-1(VSVg) as described above. DNA was isolated using the DNeasy 96 Blood & Tissue kit (Qiagen) and quantitated using Quant-iT PicoGreen R dsDNA Assay Kit (Life Technologies). Proviral DNA content was measured using Alu-PCR and total HIV DNA using internal PCR primers as described in (Butler et al., 2001; König et al., 2008; O'Doherty et al., 2002) using an Applied Biosystems 7500 Fast Real Time PCR system. All tested siRNAs were compared to a set of three scrambled negative control siRNAs analyzed in parallel. All siRNAs were tested in three independent biological replicates, and each biological replicate was assayed twice. DNA oligonucleotides used are summarized in a table below.

Oligonucleotides used for viral DNA quantification.

Primer	Oligonucleotide sequence	Position
HIV LTR (R) Forward	GCCTCAATAAAGCTTGCCTTGA	522:543 in R
HIV LTR (U5) Reverse	TCCACACTGACTAAAAGGGTCTGA	599:622 in U5
Alu Forward	GCCTCCCAAAGTGCTGGGATTACAG	in human genome
HIV Gag Reverse	GCTCTCGCACCCATCTCTCTCC	782:803 bridges beginning of gag
LTR Molecular Beacon	FAM-GCGAGTGCCCGTCT GTTGTGTGACTCTGGTAACTAGCTCGC-Dabcyl	

To quantify HIV mRNA levels samples were prepared and analyzed by qPCR using the Fast SYBR Green Cells-to-Ct Kit (Life Technologies). The primer pair 5'-TGTGTGCCCGTCTGTTGTGT-3' and 5'-GAGTCCTGCGTCGAGAGATC-3' was used to detect HIV-1 late RT product. mRNA levels were normalized to the cellular gene *GAPDH* using the primer pair 5'-CATGAGAAGTATGACAACAGCCT-3' and 5'-AGTCCTTCCACGATACCAAAGT-3'.

Cell cycle analysis. HEK293T cells were transfected with siRNAs, collected three days post transfection and fixed in absolute ethanol at -20°C overnight. Cells were washed twice with DPBS and resuspended in 3.8 mM sodium citrate, 40 µg/ml propidium iodide, and 0.5 µg/ml RNase A in DPBS. After incubating at 4°C for 3 hours, flow cytometry was performed on a BD FACScan (BD Biosciences).

Chemical compounds. Synthesis of SBI-0637142 was performed as previously described (Vamos et al., 2013). LCL161 (Weisberg et al., 2010) and TL32711 (Birinapant) (Condon et al., 2014) were obtained from ChemieTek. GDC-0152 (Flygare et al., 2012) was obtained from Santa Cruz Biotechnology. Bryostatin was purchased from Sigma-Aldrich. Vorinostat (suberanilohydroxamic acid, SAHA) and panobinostat were purchased from LC Laboratories and Fisher Scientific, respectively. All compounds were dissolved in dimethyl sulfoxide (DMSO, Fisher Scientific). Equal concentrations of DMSO were used as negative control.

Western blot analysis. To analyze whole cell lysates, cells were lysed in radioimmunoprecipitation assay (RIPA) buffer. Cytoplasmic extracts were prepared by incubating cells in Buffer A (10 mM HEPES, pH 7.9, 10 mM KCl, 0.1 mM EDTA, 1 mM dithiothreitol, 1 mM phenylmethylsulfonyl fluoride, and protease inhibitors (Sigma Aldrich)). The cells were incubated on ice for 15 min. Next, 10% Nonidet P-40 was added to a final concentration of 0.5% and the suspension was vortexed for 10 s. Cytoplasmic extracts were collected after pelleting nuclei by centrifugation. Nuclear extracts were prepared by washing isolated nuclei twice using Buffer A, followed by incubation in Buffer B (20 mM HEPES, pH 7.9, 400 mM KCl, 1 mM EDTA, 1 mM dithiothreitol, 1 mM phenylmethylsulfonyl fluoride, and protease inhibitors (Sigma Aldrich)) for 15 min on ice. After centrifugation at 20,000 rcf for 10 min the supernatants were collected as nuclear extracts. Protein concentrations of all extracts were determined using the Pierce BCA Protein Assay Kit (Life Technologies) and Western blot analysis was conducted following standard protocols. Primary antibodies against NIK (#4994), p100/p52 (#4882), IκBα (#9242), RELB (#4922), HSP90 (#4874), COX4 (#4850), and β-actin (#4970) were purchased from Cell Signaling. Primary antibodies against PARP1 (sc-8007) and RELA (sc-8008) were purchased from Santa Cruz Biotechnology. Antibodies recognizing BIRC2 (AF8181) and BIRC2/BIRC3 (MAB3400, clone 315301) were obtained from R&D Systems. An antibody against GAPDH (TA802519, clone 2D9) was purchased from OriGene. Secondary antibodies against mouse, rabbit, and goat IgG were purchased from LI-COR Biosciences and Bio-Rad. Western blots were analyzed by detection of chemiluminescence or using a LI-COR Odyssey CLx Imager.

HIV-1 infection of Human CD4+ T cells. Peripheral blood mononuclear cells (PBMCs) were isolated by Ficoll density gradient centrifugation (Histopaque, Sigma Aldrich) from buffy coats of healthy human donors (San Diego Blood Bank). CD4+ T cells were subsequently isolated by negative selection using magnetic beads (CD4+ T cell isolation kit II; Miltenyi Biotec). CD4+ T cells were cultured in RPMI1640 supplemented with 10% FBS, 100 IU penicillin, 100 µg/ml streptomycin, 0.1 M HEPES, 2 mM L-glutamine, and 20 units/ml interleukin-2 (IL-2) (NIH AIDS Reagent Program). Cells were activated with 4 µg/ml phytohemagglutinin-P (PHA) (Sigma) for 48 hours. Activated CD4+ T cells were treated with SBI-0637142, LCL-161, DMSO, or mock treated for 24 hours prior to infection with HIV-1(VSVg). Luciferase expression levels were determined using Bright-Glo Luciferase Assay System (Perkin Elmer). Cell viability of treated cells was determined using ATPlite cell viability assay (Perkin Elmer). Values were normalized to mock-treated cells; average value of DMSO-treated cells was defined as 1.

cDNA overexpression. Complementary DNA of CD40 or LTβR in the expression vector pLX304 was transfected into HEK293T cells using Lipofectamine 2000 transfection reagent (Life Technologies) according to the manufacturer's instructions. 24 hours after transfection cells were infected with HIV-1(VSVg) for 24 hours prior to the analysis of luciferase expression levels using the Bright-Glo Luciferase Assay System (Perkin Elmer).

Chromatin Immunoprecipitation: 2D10 cells were stimulated with 1 µM SBI-0637142 or DMSO for 9 h or with 20 ng of human TNFα for 2 h as a control. Cross-linking was carried out using a two-step method as previously described (Nowak et al., 2005). Cells were then lysed in RIPA buffer supplemented with protease and phosphatase inhibitor cocktails (Sigma Aldrich). Total cell lysates were extensively sonicated using a Covaris S220 Focused Ultrasonicator. Lysates were then cleared by centrifugation and supernatants were diluted 10X in RIPA buffer without SDS. Immunoprecipitations were carried out as previously described (Carey et al., 2009). The diluted whole cell lysates were incubated with Dynabeads protein G (Life Technology) and anti-RELB or anti-RELA antibodies (sc-226 and sc-372, Santa Cruz Biotechnology), or a rabbit anti-human IgG control overnight at 4°C. IP samples were washed with four different buffers according to the protocol (Carey et al., 2009). To revert the cross-link, eluted samples were incubated overnight at 65°C in the presence of 0.3 M NaCl. DNA fragments were precipitated in phenol-chloroform and DNA pellets were reconstituted in water. Samples were prepared and analyzed by qPCR. Primer pairs were designed to span the NF-κB binding site-containing region of the HIV-1 LTR, the promoter region of IκBα, or an intergenic region upstream of the *PABPC1* gene unknown to contain NF-κB binding sites as negative control. The following primer sequences were used: 5'-AGGTTTGACAGCCGCCTA-3' and 5'-AGAGACCCAGTACAGGCAAAA-3' for the HIV-1 LTR, 5'-GACGACCCCAATTCAAATCG-3' and 5'-TCAGGCTCGGGGAATTTCC-3' for the IκBα promoter, and 5'-CATGGGTGGAGCTGGTCAAT-3' and 5'-TCCTAGCAGAGATCCATGCAGAT-3' for the negative control.

Knockout cell lines: *NIK* and *NFKB2* knockout cells were generated using the Cas9 nuclease system. sgRNAs oligos were designed using the CRISPR design tool (http://tools.genome-engineering.org) and were

cloned into the pSpCas9(BB) vector as previously described (Ran et al., 2013). Sorting of transfected cells by FACS was carried out by co-expressing pSpCas9(BB) containing the specific sgRNAs oligos with the pmCherry-C1 vector. The sgRNA sequences used to knock out *NIK* or *NFKB2* were: 5' – CGTCTACAAGCTTGAGGCCG – 3' specific for exon 2 of the *NIK* gene (NG_033823.1 – 31417 to 31436), and 5' – CTTCACAGCCATATCGAAAT – 3' specific for exon 5 of the *NFKB2* gene (NG_033874.1 – 7627 to 7646).

Jurkat HIV latency model. JLat 10.6 cells (Jordan et al., 2003) from Dr. Eric Verdin were obtained through the NIH AIDS Reagent Program, Division of AIDS, NIAID, NIH. 5A8 cells (Chan et al., 2013; Sakane et al., 2011; Spina et al., 2013) were obtained from Dr. Warner C. Greene (Gladstone Institutes), and 2D10 cells (Pearson et al., 2008) from Dr. Jonathan Karn (Case Western Reserve University). Latently infected Jurkat cells were treated with compounds and subsequently analyzed for GFP expression by flow cytometry using a BD LSRFortessa cell analyzer with high throughput sampler (BD Biosciences). Cell viability was determined using the ATPlite cell viability assay (Perkin Elmer).

Analysis of drug synergy. The Bliss independence score (Bliss, 1939) was used to calculate the expected level of latency reversal when combined treatment with drugs A and B is additive. The Bliss Score was calculated using $F_{AB} = F_A + F_B * (1 – F_A)$ where F_A and F_B represent the fraction of GFP+ cells reactivated upon treatment with drug A and drug B alone and F_{AB} represents the fraction of GFP+ cells reactivated upon combined treatment with drug A and drug B. Synergy was calculated as follows: Synergy = $Observed_{AB} / F_{AB}$ where $Observed_{AB}$ represents the fraction of GFP+ cells observed upon combined treatment with drug A and drug B.

Treatment of resting CD4+ T cells from aviremic HIV patients. LRA activity of compounds was evaluated using the recently described REVEAL (rapid *ex vivo* evaluation of anti-latency) assay (Spivak et al., 2015). Aviremic HIV-1 infected patients on ART were recruited for phlebotomy according to an approved institutional review board protocol at the University of Utah (Spivak et al., 2015). Inclusion criteria mandated viral suppression (less than 50 HIV-1 RNA copies/mL) for a minimum of six months, ART initiation during chronic HIV-1 infection (greater than six months since seroconversion) and compliance with a stable ART regimen for a minimum of twelve months per participant and provider report. Informed consent and phlebotomy were performed in the Center for Clinical and Translational Science Clinical Services Core at the University of Utah Medical Center.

Peripheral blood mononuclear cells were isolated from whole blood immediately after phlebotomy via density gradient centrifugation, followed by negative selection of resting CD4+ T cells using magnetic bead separation (Miltenyi Biotec and StemCell Technologies). Aliquots of $5x10^6$ resting CD4+ T cells were cultured under multiple conditions: culture medium and DMSO (solvent) alone (negative control), CD3/CD28 antibody-coated magnetic beads (positive control) and medium containing candidate latency reversing agents at concentrations previously shown to induce viral reactivation. At 48 hours culture supernatants were collected for real time quantitative polymerase chain reaction (qPCR). Supernatant from each sample was collected for

quantification of cell-free virions using a two-step qPCR that makes use of a primer and probe set for conserved regions of the 3' LTR of HIV-1 mRNA (Shan et al., 2013).

Analysis of resting CD4+ T cell activation. Resting CD4+ T cells isolated from the blood of healthy donors were treated with DMSO, 10 μM SBI-0637142, 100 nM panobinostat, 30 nM bryostatin, or CD3/CD28 antibody-coated magnetic beads for 48 hours. Cells were stained with PE-labeled anti-CD69 antibody sc-18880PE (Santa Cruz Biotechnology) and analyzed by FACS.

SUPPLEMENTAL REFERENCES

Bliss, C.I. (1939). The toxicity of poisons applied jointly. Annals of Applied Biology *26*, 585-615.

Butler, S.L., Hansen, M.S., and Bushman, F.D. (2001). A quantitative assay for HIV DNA integration in vivo. Nature medicine *7*, 631-634.

Carey, M.F., Peterson, C.L., and Smale, S.T. (2009). Chromatin immunoprecipitation (ChIP). Cold Spring Harbor protocols *2009*, pdb prot5279.

Chan, J.K., Bhattacharyya, D., Lassen, K.G., Ruelas, D., and Greene, W.C. (2013). Calcium/calcineurin synergizes with prostratin to promote NF-kappaB dependent activation of latent HIV. PloS one *8*, e77749.

Condon, S.M., Mitsuuchi, Y., Deng, Y., Laporte, M.G., Rippin, S.R., Haimowitz, T., Alexander, M.D., Kumar, P.T., Hendi, M.S., Lee, Y.H.*, et al.* (2014). Birinapant, a Smac-Mimetic with Improved Tolerability for the Treatment of Solid Tumors and Hematological Malignancies. Journal of medicinal chemistry.

Flygare, J.A., Beresini, M., Budha, N., Chan, H., Chan, I.T., Cheeti, S., Cohen, F., Deshayes, K., Doerner, K., Eckhardt, S.G.*, et al.* (2012). Discovery of a potent small-molecule antagonist of inhibitor of apoptosis (IAP) proteins and clinical candidate for the treatment of cancer (GDC-0152). Journal of medicinal chemistry *55*, 4101-4113.

Jordan, A., Bisgrove, D., and Verdin, E. (2003). HIV reproducibly establishes a latent infection after acute infection of T cells in vitro. The EMBO journal *22*, 1868-1877.

König, R., Chiang, C.Y., Tu, B.P., Yan, S.F., DeJesus, P.D., Romero, A., Bergauer, T., Orth, A., Krueger, U., Zhou, Y.*, et al.* (2007). A probability-based approach for the analysis of large-scale RNAi screens. Nature methods *4*, 847-849.

Nowak, D.E., Tian, B., and Brasier, A.R. (2005). Two-step cross-linking method for identification of NF-kappaB gene network by chromatin immunoprecipitation. BioTechniques *39*, 715-725.

O'Doherty, U., Swiggard, W.J., Jeyakumar, D., McGain, D., and Malim, M.H. (2002). A sensitive, quantitative assay for human immunodeficiency virus type 1 integration. J Virol *76*, 10942-10950.

Ran, F.A., Hsu, P.D., Wright, J., Agarwala, V., Scott, D.A., and Zhang, F. (2013). Genome engineering using the CRISPR-Cas9 system. Nature protocols *8*, 2281-2308.

Sakane, N., Kwon, H.S., Pagans, S., Kaehlcke, K., Mizusawa, Y., Kamada, M., Lassen, K.G., Chan, J., Greene, W.C., Schnoelzer, M.*, et al.* (2011). Activation of HIV transcription by the viral Tat protein requires a demethylation step mediated by lysine-specific demethylase 1 (LSD1/KDM1). PLoS pathogens *7*, e1002184.

Shan, L., Rabi, S.A., Laird, G.M., Eisele, E.E., Zhang, H., Margolick, J.B., and Siliciano, R.F. (2013). A novel PCR assay for quantification of HIV-1 RNA. J Virol *87*, 6521-6525.

Spina, C.A., Anderson, J., Archin, N.M., Bosque, A., Chan, J., Famiglietti, M., Greene, W.C., Kashuba, A., Lewin, S.R., Margolis, D.M.*, et al.* (2013). An in-depth comparison of latent HIV-1 reactivation in multiple cell model systems and resting CD4+ T cells from aviremic patients. PLoS pathogens *9*, e1003834.

Weisberg, E., Ray, A., Barrett, R., Nelson, E., Christie, A.L., Porter, D., Straub, C., Zawel, L., Daley, J.F., Lazo-Kallanian, S.*, et al.* (2010). Smac mimetics: implications for enhancement of targeted therapies in leukemia. Leukemia *24*, 2100-2109.